



EUROfusion

WP14ER-PR(18) 19317

F Deluzet et al.

**A two field iterated
Asymptotic-Preserving for highly
anisotropic elliptic equations**

Preprint of Paper to be submitted for publication in
Multiscale Modeling and Simulation



This work has been carried out within the framework of the EUROfusion Consortium and has received funding from the Euratom research and training programme 2014-2018 under grant agreement No 633053. The views and opinions expressed herein do not necessarily reflect those of the European Commission.

This document is intended for publication in the open literature. It is made available on the clear understanding that it may not be further circulated and extracts or references may not be published prior to publication of the original when applicable, or without the consent of the Publications Officer, EUROfusion Programme Management Unit, Culham Science Centre, Abingdon, Oxon, OX14 3DB, UK or e-mail Publications.Officer@euro-fusion.org

Enquiries about Copyright and reproduction should be addressed to the Publications Officer, EUROfusion Programme Management Unit, Culham Science Centre, Abingdon, Oxon, OX14 3DB, UK or e-mail Publications.Officer@euro-fusion.org

The contents of this preprint and all other EUROfusion Preprints, Reports and Conference Papers are available to view online free at <http://www.euro-fusionscipub.org>. This site has full search facilities and e-mail alert options. In the JET specific papers the diagrams contained within the PDFs on this site are hyperlinked

1 **A TWO FIELD ITERATED ASYMPTOTIC-PRESERVING METHOD**
 2 **FOR HIGHLY ANISOTROPIC ELLIPTIC EQUATIONS**

3 FABRICE DELUZET * AND JACEK NARSKI*

4 **Abstract.** A new two field iterated Asymptotic-Preserving method is introduced for the numeri-
 5 cal resolution of strongly anisotropic elliptic equations. This method does not rely on any integration
 6 of the field defining the anisotropy. It rather harnesses an auxiliary variable removing any stiffness
 7 from the equation. Compared to precedent realizations using the same approach, the iterated method
 8 allows for the resolution of each field independently within an iterative process to converge the two
 9 unknowns. This brings advantages in the computational efficiency of the method for large meshes, a
 10 better scaling of the matrices condition number with respect to the mesh refinement as well as the
 11 ability to address complex anisotropy topology including closed field lines.

12 **Key words.** Anisotropic diffusion, asymptotic preserving scheme, iterative method

13 **AMS subject classifications.** 65N30

14 **1. Introduction.** The present paper is aimed at introducing a new Asymptotic-
 15 Preserving scheme for the resolution of singular perturbation problems stemming
 16 from strongly anisotropic elliptic equations. This type of equations are representative
 17 of plasma physics evolution under large magnetic fields such as Tokamak plasmas
 18 [8, 9]. Here the focus is made on a simplified model problem containing the main
 19 difficulty characterizing these equations but without all the complexity of the physical
 20 background. This simplified context allows the construction of analytic solutions
 21 which are used to assess the effectiveness of the numerical method introduced herein.
 22 Let b denote the vector field providing the direction of the magnetic field, b verifying
 23 $|b| = 1$, the model problem writes

$$24 \quad (1) \quad \begin{cases} -\nabla \cdot (\mathbb{A}_\varepsilon \nabla u^\varepsilon) = f^\varepsilon & \text{in } \Omega, \\ n \cdot \mathbb{A}_\varepsilon \nabla u^\varepsilon = 0 & \text{on } \Gamma_N, \\ u^\varepsilon = 0 & \text{on } \Gamma_D, \end{cases}$$

25
 26 where n is the outward normal to the domain, $\Gamma_N \cup \Gamma_D$ the domain boundary, with
 27 $b \cdot n = 0$ on Γ_D and $b \cdot n \neq 0$ on Γ_N . The anisotropy of the problem is defined by the
 28 diffusion matrix \mathbb{A}_ε related to the vector field b by two positive functions A_\parallel and A_\perp
 29 with

$$30 \quad (2) \quad \mathbb{A}_\varepsilon = \frac{1}{\varepsilon} A_\parallel b \otimes b + (\mathbb{Id} - b \otimes b) A_\perp (\mathbb{Id} - b \otimes b).$$

31
 32 In this equation \mathbb{Id} is the identity matrix, the tensor product being denoted \otimes . The
 33 parameter ε^{-1} defines the strength of the anisotropy.

34 The difficulty addressed in this paper is related to the singular nature of the
 35 problem. Indeed in the limit of infinite anisotropy strength ($\varepsilon \rightarrow 0$) the system
 36 (1) is degenerate. Indeed, the differential operator in the elliptic equation reduces
 37 to the dominant operator (the derivatives carried by ε^{-1} in (1)) which is supplied
 38 with Neumann like boundary conditions. This degenerate system admits an infinite
 39 amount of solutions, any function with no gradient along b being in the kernel of the
 40 dominant operator.

*Université de Toulouse, UPS, INSA, UT1, UTM, Institut de Mathématiques de Toulouse, F-31062 Toulouse, France

41 The derivation of efficient numerical methods for the approximation of this class
42 of problems is a difficult task. The straight discretization of (1) gives rise to sys-
43 tem matrices with condition number blowing up with the increase of the anisotropy
44 strength. This is outlined in precedent works (see [10] for numerical investigations
45 or [15] and [22] for an analysis). Therefore these approaches are limited to reduced
46 anisotropy strength.

47 A way to circumvent this difficulty is to develop Asymptotic-Preserving methods
48 as introduced in [14] for a different context. Actually a well posed system can be
49 derived to compute uniquely the solution in the limit of infinite parallel diffusion. The
50 aim of such method is to guarantee that the discrete system is consistent with this
51 well posed problem for vanishing ε rather than with the degenerate one. This ensures
52 that the condition number of the system matrix remains bounded independently of
53 the anisotropy strength.

54 In precedent works, different AP schemes have been derived for this class of prob-
55 lems. The first iterations were devoted to anisotropy directions aligned with one
56 coordinate [10, 5]. This requirement has been released in [11] and extended to closed
57 field lines in [16]. In all these works the problem is reformulated into a two field prob-
58 lem based on a decomposition of the solution into a microscopic and a macroscopic
59 component. This reformulated two field system offers the advantage of embedding the
60 limit problem. Hence, the limit $\varepsilon \rightarrow 0$ is a regular limit in this set of equations. How-
61 ever the decomposition of the solution is not unique and different numerical methods
62 can be derived according to the choices implemented in this reformulated system.
63 The present work aims at exploring further the possibilities offered by a different
64 decomposition. Note that the method developed herein does not rely on any geomet-
65 rical procedure, requiring an integration along the b -field lines as proposed by other
66 authors [6, 19].

67 The main goal of the present work is to correct some of the weaknesses of the
68 precedent realizations. The first one is related to the structure of the discrete system
69 issued from the discretization of the reformulated problem. So far, this system strongly
70 couples the equations providing both components and is therefore solved at once. We
71 propose a different method referred to as “two field iterated Asymptotic-Preserving”
72 method which offers the ability to solve each component independently, in an itera-
73 tive process. The system solved for each component is the same mildly anisotropic
74 problem parameterized by a numerical parameter $\varepsilon_0 \gg \varepsilon$ with different source term
75 for every component. This gains an improved efficiency in terms of computational
76 resources compared to the direct resolution of the two field system. A second advan-
77 tage of this new method is related to the conditioning of the system matrix. The
78 linear systems issued from precedent AP methods [11, 15] have a condition number
79 scaling as $1/h^4$, h denoting the typical mesh size. The two field iterated method intro-
80 duced herein requires only the resolution of linear systems with a condition number
81 scaling as $1/(\varepsilon_0 h^2)$. An additional advantage is the ability to carry out numerical
82 approximations with closed field lines. This is a difficulty that can not be addressed
83 by the Micro-Marco AP scheme [11]. Indeed this numerical method requires that all
84 the field lines cross the domain boundary. It should be pointed out that a solution
85 has been proposed in [16] in the frame of the “stabilized” Micro-Macro scheme. It
86 consists in introducing a stabilization operator small enough not to deteriorate the
87 precision of the numerical method. The main difficulty with this approach lies in the
88 choice of the stabilization operator scaling. Indeed, it should be kept large enough to
89 preserve a good conditioning of the system matrix but small enough to be comparable
90 to the truncation error of the discretizations. This prevents from using the stabilized

91 method with high order methods. The two field iterated method is free from these
 92 weaknesses. We also show that, the parameter ε_0 can be chosen in a wide range of
 93 values preventing the so-called locking effect [4] and securing a fast convergence of the
 94 iterations as well as a good conditioning of the linear systems. The numerical method
 95 is also free from the perpendicular dynamic pollution by the parallel one, reported by
 96 other authors in very similar frameworks [12, 13, 20, 21].

97 The outlines of the paper are the following. The problem at hand in the present
 98 work is stated in Section 2 with highlights on the singular nature of the limit $\varepsilon \rightarrow 0$.
 99 The two field iterated AP method is then introduced and the convergence of the it-
 100 erative procedure is demonstrated. Finally, emphasizes are made on how this new
 101 method compares to precedent works. Numerical investigations are carried out in
 102 Section 3. Different setups are proposed to asses the effectiveness of the method.
 103 The locking effect is first investigated and the robustness of the method with respect
 104 to this classical issue is outlined. The efficiency of the two field iterated method is
 105 benchmarked against the Micro-Macro scheme. This demonstrates tremendous gains
 106 for large meshes. Two other test cases are finally proposed. The second one is a dif-
 107 fusion in a ring similarly to computations performed in [7, 18] but proposed here with
 108 anisotropy strength much more severe. The last test case is aimed at demonstrating
 109 the ability to carry out accurate numerical approximations in frameworks including
 110 closed field lines.

111 2. The anisotropic problem and its asymptotic-preserving formulation.

112 **2.1. Introduction and notations.** Let $b \in (C^\infty(\bar{\Omega}))^d$ be a smooth vector field
 113 in a domain $\Omega \subset \mathbb{R}^d$, with $d = 2, 3$ and $|b(x)| = 1$ for all $x \in \Omega$. Let us also decompose
 114 the boundary $\Gamma = \partial\Omega$ into two parts: Γ_D parallel to b and its complement Γ_N :

$$115 \quad (3) \quad \Gamma_D = \{x \in \Gamma \mid b(x) \cdot n = 0\}, \quad \Gamma_N = \Gamma \setminus \Gamma_D,$$

117 where n is the outward normal to Ω . Let us also decompose any vector $v \in \mathbb{R}^d$,
 118 gradients $\nabla\phi$, with $\phi(x)$ a scalar function, and divergence $\nabla \cdot v$ into a part parallel to
 119 the anisotropy direction and a part perpendicular to it with:

$$\begin{aligned} 120 \quad v_{\parallel} &:= (v \cdot b)b, & v_{\perp} &:= (\text{Id} - b \otimes b)v, & \text{such that } v &= v_{\parallel} + v_{\perp}, \\ \nabla_{\parallel}\phi &:= (b \cdot \nabla\phi)b, & \nabla_{\perp}\phi &:= (\text{Id} - b \otimes b)\nabla\phi, & \text{such that } \nabla\phi &= \nabla_{\parallel}\phi + \nabla_{\perp}\phi, \\ \nabla_{\parallel} \cdot v &:= \nabla \cdot v_{\parallel}, & \nabla_{\perp} \cdot v &:= \nabla \cdot v_{\perp}, & \text{such that } \nabla \cdot v &= \nabla_{\parallel} \cdot v + \nabla_{\perp} \cdot v, \end{aligned}$$

121 where we denoted Id the identity matrix and \otimes the vector tensor product. The
 122 following notations and definitions will be helpful in the sequel.

123 **DEFINITION 1.** Let \mathcal{V} and \mathcal{G} be the functional spaces defined by

$$124 \quad (4) \quad \mathcal{V} = \{v \in H^1(\Omega) : v|_{\Gamma_D} = 0\},$$

$$125 \quad (5) \quad \mathcal{G} = \{v \in \mathcal{V} : \nabla_{\parallel}v = 0\}.$$

127 For any function $\phi \in \mathcal{V}$, $\varepsilon_0 \in \mathbb{R}$, $\varepsilon_0 > 0$, $A_{\parallel} \in C^\infty(\bar{\Omega})$ a positive function and
 128 $A_{\perp} \in \mathbb{M}_{d \times d}(C^\infty(\bar{\Omega}))$ a matrix satisfying

$$130 \quad (6) \quad A_0 \|v\|^2 \leq v^T A_{\perp} v \leq A_1 \|v\|^2, \quad \forall v \in \mathbb{R}^d$$

131 for some positive constants A_0 and A_1 , we introduce the operators Δ_{\parallel} , Δ_{\perp} and Δ_{ε_0}

132 defined as

$$133 \quad (7a) \quad \Delta_{\parallel} \phi = \nabla_{\parallel} \cdot (A_{\parallel} \nabla_{\parallel} \phi) ,$$

$$134 \quad (7b) \quad \Delta_{\perp} \phi = \nabla_{\perp} \cdot (A_{\perp} \nabla_{\perp} \phi) ,$$

$$135 \quad (7c) \quad \Delta_{\varepsilon_0} \phi = \Delta_{\parallel} \phi + \varepsilon_0 \Delta_{\perp} \phi ;$$

137 and for $(u, v) \in \mathcal{V} \times \mathcal{V}$ the associated bilinear forms

$$138 \quad (8a) \quad a_{\parallel}(u, v) = \int_{\Omega} A_{\parallel} \nabla_{\parallel} u \cdot \nabla_{\parallel} v dx ,$$

$$139 \quad (8b) \quad a_{\perp}(u, v) = \int_{\Omega} (A_{\perp} \nabla_{\perp} u) \cdot \nabla_{\perp} v dx .$$

141 Finally the matrix $\mathbb{A}_{\varepsilon_0}$ is introduced with

$$142 \quad (9a) \quad \mathbb{A}_{\varepsilon_0} = \mathbb{A}_{\parallel} (b \otimes b) + \varepsilon_0 (\text{Id} - b \otimes b) \mathbb{A}_{\perp} (\text{Id} - b \otimes b)$$

143 and the induced norm

$$144 \quad (9b) \quad \|u\|_{\varepsilon_0}^2 = a_{\parallel}(u, u) + \varepsilon_0 a_{\perp}(u, u) .$$

146 **2.2. The singular perturbation problem.** The problem studied in this paper
147 is the following: find u^{ε} such that

$$148 \quad (10) \quad \begin{cases} -\frac{1}{\varepsilon} \Delta_{\parallel} u^{\varepsilon} - \Delta_{\perp} u^{\varepsilon} = f & \text{in } \Omega, \\ \frac{1}{\varepsilon} n_{\parallel} \cdot (A_{\parallel} \nabla_{\parallel} u^{\varepsilon}) + n_{\perp} \cdot (A_{\perp} \nabla_{\perp} u^{\varepsilon}) = 0 & \text{on } \Gamma_N, \\ u^{\varepsilon} = 0 & \text{on } \Gamma_D, \end{cases}$$

150 This problem is referred to as a singular perturbation problem, because of its degeneracy for vanishing ε . Indeed, setting ε to 0 in (10), the problem reduces to

$$152 \quad (11) \quad \begin{cases} -\Delta_{\parallel} u^0 = 0 & \text{in } \Omega, \\ n_{\parallel} \cdot (A_{\parallel} \nabla_{\parallel} u^0) = 0 & \text{on } \Gamma_N, \\ u^0 = 0 & \text{on } \Gamma_D, \end{cases}$$

154 which admits an infinite number of solutions as any function v that is constant in the
155 direction of anisotropy ($v \in \mathcal{G}$) solves this problem. The limit of the solution can be
156 computed by multiplying (10) by a test function $v \in \mathcal{G}$, integrating by parts over Ω
157 and then let $\varepsilon \rightarrow 0$. This leads to the following, well posed problem: find $u^0 \in \mathcal{G}$ such
158 that

$$159 \quad (12) \quad \int_{\Omega} (A_{\perp} \nabla_{\perp}) u^0 \cdot \nabla_{\perp} v = \int_{\Omega} f v , \quad \forall v \in \mathcal{G} ,$$

161 which defines a weak formulation of the limit problem. The difficulty when dealing
162 with the numerical approximation of (1) consists in imposing the consistency of the
163 scheme with the limit problem (12) rather than the degenerate one (11) when $\varepsilon \rightarrow 0$.
164 Standard discretizations of the problem (10) are not compliant with this property. The
165 condition number of the associated system matrices are increasing with the anisotropy

166 strength ε^{-1} . This translates that the numerical methods provide a discretization of
 167 the degenerate problem for vanishing ε -values. To address this issue, the philosophy
 168 of Asymptotic Preserving schemes relies on a discretization of a suitable reformulated
 169 problem. This system is equivalent to the problem (10) for $\varepsilon > 0$, however the limit
 170 problem (12) is recovered from the reformulated system when ε is set to 0.

171 Another difficulty encountered when dealing with the numerical resolution of
 172 anisotropic problems is the so-called locking phenomenon [4]. To highlight this issue in
 173 the present framework, let us again consider the reduced problem (11). This problem
 174 states that the solution has no gradient along b for vanishing ε . If the discrete space
 175 does not contain functions that are constant in the direction of the anisotropy, then
 176 the numerical approximation of this problem does not converge to the solution of the
 177 problem. It is important to point out that the locking is not related to the fact that the
 178 reduced problem is ill posed on the continuous level but to the coarse approximation
 179 properties of the discrete functional space. That is the case, for example, when
 180 either unstructured (triangular) meshes or rectangular Cartesian grids with variable
 181 anisotropy directions are used with low order numerical methods. For small non zero
 182 values of ε , large enough to preserve a good conditioning of the matrix related to the
 183 discretized version of the (10), the locking phenomenon is manifested in the discrete
 184 solution converging to zero as ε gets smaller. This feature will be illustrated in the
 185 section devoted to the numerical investigations.

186 **2.3. A two field iterated Asymptotic-Preserving method.** Let us now
 187 propose a two step iterative method to solve the singular perturbation problem (10).
 188 Let us consider $\tilde{\varepsilon}_0$ smaller than one but big enough so that the singular perturbation
 189 problem for $\varepsilon = \tilde{\varepsilon}_0$ is not yet singular nor the discretized system suffers from locking.
 190 Let us define $\varepsilon_0 = \max\{\tilde{\varepsilon}_0, \varepsilon\}$ so that ε_0 is never smaller than ε .

191 Let us first observe that the source of the numerical issues in the resolution
 192 of the original problem (10) is the dominant derivative, multiplied by ε^{-1} , in the
 193 direction of the anisotropy. The idea behind the herein proposed scheme relies on the
 194 introduction of an additional variable that fulfils the following relation: $\varepsilon\Delta_{\parallel}q = \Delta_{\parallel}u$.
 195 This operation allows to eliminate the stiff term from the equation, preventing by this
 196 means the degeneracy of the equation. The two field system becomes:

$$197 \quad (13) \quad \begin{cases} -\Delta_{\parallel}q - \Delta_{\perp}u = f, \\ -\Delta_{\parallel}u = -\varepsilon\Delta_{\parallel}q, \end{cases}$$

199 supplied with the boundary conditions precised in (10) for both u and q . This system
 200 does not have a unique solution as q is defined up to a function constant in the
 201 direction of the anisotropy. Let us now multiply the first equation by ε_0 and add it
 202 to the second one to get:

$$203 \quad (14) \quad -\Delta_{\varepsilon_0}u = \varepsilon_0f + (\varepsilon_0 - \varepsilon)\Delta_{\parallel}q,$$

204 allowing to compute u uniquely if q is known. The next step consists in decoupling
 205 the problems and solve the two resulting equations in an iterative manner, finding
 206 first an approximation to u using q computed in the previous step, then recompute q
 207 and repeat until convergence. This yields the following iterations

$$208 \quad (15) \quad \begin{cases} -\Delta_{\varepsilon_0}u^{n+1} = \varepsilon_0f + (\varepsilon_0 - \varepsilon)\Delta_{\parallel}q^n, \\ -\Delta_{\parallel}q^{n+1} = f + \Delta_{\perp}u^{n+1}. \end{cases}$$

210 The second equation of this iterative scheme is not yet invertible. Let us now add
 211 the term $-\varepsilon_0\Delta_{\perp}q^{n+1}$ to the left hand side and subtract its equivalent for q^n from the

212 left hand side. The resulting problem for q^{n+1} has a unique solution for given q^n and
 213 u^{n+1} . Finally, the two field iterated method is defined in the following way:

$$214 \quad (16) \quad \begin{cases} -\Delta_{\varepsilon_0} u^{n+1} = \varepsilon_0 f + (\varepsilon_0 - \varepsilon) \Delta_{\parallel} q^n & \text{in } \Omega, \\ n \cdot \mathbb{A}_{\varepsilon_0} \nabla u^{n+1} = -(\varepsilon_0 - \varepsilon) n \cdot (A_{\parallel} \nabla_{\parallel} q^n) & \text{on } \Gamma_N, \\ u^{n+1} = 0 & \text{on } \Gamma_D, \end{cases}$$

$$215 \quad (17) \quad \begin{cases} -\Delta_{\varepsilon_0} q^{n+1} = f + \Delta_{\perp} (u^{n+1} - \varepsilon_0 q^n) & \text{in } \Omega, \\ n \cdot \mathbb{A}_{\varepsilon_0} \nabla q^{n+1} = -n \cdot (A_{\perp} \nabla_{\perp} (u^{n+1} - \varepsilon_0 q^n)) & \text{on } \Gamma_N, \\ q^{n+1} = 0 & \text{on } \Gamma_D, \end{cases}$$

217 where q^{n+1} is an auxiliary variable and u^{n+1} the approximation to u^ε . In this method,
 218 the original strongly anisotropic elliptic problem (10) is replaced by a set of two only
 219 mildly anisotropic equations parameterized by $\varepsilon_0 \gg \varepsilon$. Moreover, the matrix to be
 220 inverted in the first step (16) of the iterative method is the same as in the final step
 221 (17), the only difference is in the right hand side of the equation. That is to say,
 222 the matrix has to be factorized only once, the rest of the iterative scheme is a fast
 223 triangular system solve. This method does not require any discretization of the space
 224 \mathcal{G} (functions constant in the direction of the anisotropy), which can be complicated
 225 for generic field b . To be complete, the variational formulation of the iterative scheme
 226 (16-17) is stated:

227 Find $(q^{n+1}, u^{n+1}) \in \mathcal{V}^2$ such that

$$228 \quad (18) \quad a_{\parallel}(u^{n+1}, v) + \varepsilon_0 a_{\perp}(u^{n+1}, v) = \varepsilon_0(f, v) - (\varepsilon_0 - \varepsilon) a_{\parallel}(q^n, v), \quad \forall v \in \mathcal{V},$$

$$229 \quad (19) \quad a_{\parallel}(q^{n+1}, w) + \varepsilon_0 a_{\perp}(q^{n+1}, w) = (f, w) - a_{\perp}(u^{n+1} - \varepsilon_0 q^n, w), \quad \forall w \in \mathcal{V}.$$

231 Let us now prove that the iterative scheme (16-17) converges and that the limit
 232 solution solves the original singular perturbation problem.

233 **THEOREM 2.** *For any $(q^0, u^0) \in \mathcal{V} \times \mathcal{V}$, the sequence $(q^n, u^n)_{n>0}$ defined by the*
 234 *iterative method (16-17) converges to a solution (\bar{q}, \bar{u}) . The component \bar{u} of the sta-*
 235 *tionary point solves uniquely the initial singular perturbation problem (10) for $\varepsilon > 0$*
 236 *and the limit problem (12) when $\varepsilon = 0$.*

237 To prove Theorem 2, the following lemmas and proposition are necessary.

238 **LEMMA 3.** *The operator Δ_{ε_0} is invertible on \mathcal{V} . The eigenvalues of the operator*
 239 *$\Delta_{\varepsilon_0}^{-1} \Delta_{\parallel}$ are real non negative and bounded by 1. The eigen functions ν^0 associated to*
 240 *the null eigenvalue belong to the kernel of the operator Δ_{\parallel} : $\nu^0 \in \mathcal{G}$.*

241 **LEMMA 4.** *The iterative method defined by Eqs. (16-17) yields the following re-*
 242 *urrence*

$$243 \quad (20) \quad q^{n+1} = A_I q^n - \Delta_{\varepsilon_0}^{-1} \Delta_{\parallel} \Delta_{\varepsilon_0}^{-1} f$$

245 for $n \geq 1$, the iteration operator A_I being defined as

$$246 \quad (21) \quad A_I = 1 - \frac{\varepsilon}{\varepsilon_0} \Delta_{\varepsilon_0}^{-1} \Delta_{\parallel} - \frac{\varepsilon_0 - \varepsilon}{\varepsilon_0} (\Delta_{\varepsilon_0}^{-1} \Delta_{\parallel})^2.$$

248 *The eigenvalues of A_I , denoted ℓ_i , are real with $\ell_i \in [0, 1]$. The eigenfunctions asso-*
 249 *ciated to the largest eigenvalue $\ell_i = 1$ is in the kernel of the operator Δ_{\parallel} .*

250 LEMMA 5 (Orthogonality of $q^{n+1} - q^n$ with respect to $w \in \mathcal{G}$). For any $q^0 \in \mathcal{V}$
 251 all functions in the sequence $(q^n)_{n \geq 0}$ issued from the iterative method (16-17) differ
 252 from each other only by a function orthogonal to \mathcal{G} , the space of functions constant
 253 in the direction of anisotropy with respect to the H^1 seminorm. That is to say, for
 254 any $i, j \geq 0$ the difference $q^j - q^i$ is orthogonal to \mathcal{G} with respect to the H^1 seminorm.
 255 Moreover, if $\nabla_{\perp} q^0 = 0$ than q^n is orthogonal to \mathcal{G} with respect to the H^1 seminorm
 256 for all $n \geq 0$.

257 PROPOSITION 6. For any fixed point (\bar{u}, \bar{q}) of the iterative method defined by
 258 Eqs. (16-17), the component \bar{u} is the solution of the singular perturbation problem
 259 (10) for $\varepsilon > 0$ and of the limit problem (12) for $\varepsilon = 0$.

260 *Proof of lemma 3.* The operator Δ_{ε_0} is invertible due to standard elliptic argu-
 261 ments. The eigensystem of the operator $\Delta_{\varepsilon_0}^{-1} \Delta_{\parallel}$ is defined by the problem:
 262 Find $\lambda_i \in \mathbb{R}$ and $q_i \in \mathcal{V}$ such that

$$263 \quad (22) \quad \Delta_{\varepsilon_0}^{-1} \Delta_{\parallel} q_i = \lambda_i q_i,$$

264 or equivalently

$$265 \quad (23) \quad \Delta_{\parallel} q_i = \lambda_i \Delta_{\varepsilon_0} q_i.$$

266 Multiplication by q_i (or by q_i^* , if q_i is assumed to have complex values and $\lambda_i \in \mathbb{C}$)
 267 and integration by parts yield

$$270 \quad (24) \quad \lambda_i = \frac{a_{\parallel}(q_i, q_i)}{a_{\parallel}(q_i, q_i) + \varepsilon_0 a_{\perp}(q_i, q_i)}.$$

271 Clearly all eigenvalues are real and between 0 and 1. □

272 *Proof of lemma 4.* Thanks to Eq. (16) it follows that, on the one hand

$$273 \quad (25) \quad u^{n+1} = -\varepsilon_0 \Delta_{\varepsilon_0}^{-1} f - (\varepsilon_0 - \varepsilon) \Delta_{\varepsilon_0}^{-1} \Delta_{\parallel} q^n$$

274 and, on the other hand

$$275 \quad f + \Delta_{\perp} u^{n+1} = \frac{1}{\varepsilon_0} \left(-\Delta_{\parallel} u^{n+1} - (\varepsilon_0 - \varepsilon) \Delta_{\parallel} q^n \right).$$

276 Plugging this identity into Eq. (17) yields,

$$277 \quad (26) \quad \Delta_{\varepsilon_0} q^{n+1} = \Delta_{\varepsilon_0} q^n + \frac{1}{\varepsilon_0} \Delta_{\parallel} u^{n+1} - \frac{\varepsilon}{\varepsilon_0} \Delta_{\parallel} q^n.$$

280 After some algebra and using Eq. (25), the recurrence relation (20) between q^{n+1}
 281 and q^n is recovered. The eigenvalues of the iteration operator A_I defined by Eq. (21)
 282 verify

$$283 \quad (27) \quad \ell_i = 1 - \frac{\varepsilon}{\varepsilon_0} \lambda_i - \frac{\varepsilon_0 - \varepsilon}{\varepsilon_0} \lambda_i^2$$

284 where λ_i are the eigenvalues of the operator $\Delta_{\varepsilon_0}^{-1} \Delta_{\parallel}$ characterized in lemma 3. Note
 285 that ℓ_i is a decreasing function of λ_i for $\varepsilon_0 > \varepsilon$, with $\ell_i = 1$ for $\lambda_i = 0$ and $\ell_i = 0$ for
 286 $\lambda_i = 1$. □

288 *Proof of lemma 5.* Let us first prove that $q^{n+1} - q^n$ is orthogonal to the space \mathcal{G}
 289 with respect to the H^1 seminorm. Let us plug $w \in \mathcal{G}$ into (19) to get

$$290 \quad (28) \quad \varepsilon_0 a_{\perp}(q^{n+1}, w) = (f, w) - a_{\perp}(u^{n+1}, w) + \varepsilon_0 a_{\perp}(q^n, w) \quad , \quad \forall w \in \mathcal{G}.$$

292 Owing to the identity $a_{\perp}(u^{n+1}, w) = (f, w)$ and thanks to (18) evaluated with $v =$
 293 $w \in \mathcal{G}$, the following relation is derived

$$294 \quad (29) \quad a_{\perp}(q^{n+1} - q^n, w) = 0 \quad , \quad \forall w \in \mathcal{G},$$

296 which finally leads to

$$297 \quad (30) \quad a_{\parallel}(q^{n+1} - q^n, w) + a_{\perp}(q^{n+1} - q^n, w) = 0 \quad , \quad \forall w \in \mathcal{G}.$$

299 This proves that $q^{n+1} - q^n$ is orthogonal to \mathcal{G} with respect to the H^1 seminorm. It
 300 follows immediately that $q^{n+l} - q^n$ is also orthogonal to \mathcal{G} for any $l \geq 1$ and $n \geq 0$:
 301

$$302 \quad (31) \quad a_{\parallel}(q^{n+l} - q^n, w) + a_{\perp}(q^{n+l} - q^n, w) \\
 303 \quad = \sum_{i=n}^{n+l-1} (a_{\parallel}(q^{i+1} - q^i, w) + a_{\perp}(q^{i+1} - q^i, w)) = 0 \quad , \quad \forall w \in \mathcal{G}. \quad \square$$

305 Moreover, if $\nabla_{\perp} q^0 = 0$ than q^n is orthogonal to \mathcal{G} in the H^1 seminorm.

306 *Proof of Proposition 6.* Let (\bar{q}, \bar{u}) be the stationary point of the iterative scheme.
 307 Eqs. (16) and (17) yield

$$308 \quad (32) \quad -\Delta_{\parallel} \bar{q} - \Delta_{\perp} \bar{u} = f$$

$$309 \quad (33) \quad -\Delta_{\parallel} \bar{u} - \varepsilon_0 \Delta_{\perp} \bar{u} = -\varepsilon \Delta_{\parallel} \bar{q} + \varepsilon_0 (f + \Delta_{\parallel} \bar{q})$$

311 which gives

$$312 \quad (34) \quad \Delta_{\parallel} \bar{u} = \varepsilon \Delta_{\parallel} \bar{q},$$

314 a relation that couples the parallel gradient of \bar{u} with that of \bar{q} . Combining this again
 315 with (32) one obtains the initial singular perturbation problem:

$$316 \quad (35) \quad -\frac{1}{\varepsilon} \Delta_{\parallel} \bar{u} - \Delta_{\perp} \bar{u} = f.$$

318 The boundary conditions become:

$$319 \quad (36) \quad n \cdot \nabla_{\parallel} \bar{q} = -n \cdot \nabla_{\perp} \bar{u}$$

321 and

$$322 \quad (37) \quad n \cdot \mathbb{A}_{\varepsilon_0} \nabla \bar{u} = -(\varepsilon_0 - \varepsilon) n \cdot \nabla_{\parallel} \bar{q} = (\varepsilon_0 - \varepsilon) n \cdot \nabla_{\perp} \bar{u},$$

324 which proves that the boundary conditions for the original singular perturbation prob-
 325 lem are recovered for the converged solution of the iterative scheme.

326 This problem admits a unique solution \bar{u} for $\varepsilon \neq 0$, independent on u^0 . If $\varepsilon = 0$
 327 then Eqs. (32) and (35) provide the following system:

$$328 \quad (38) \quad \begin{cases} -\Delta_{\parallel} \bar{q} - \Delta_{\perp} \bar{u} = f, \\ -\Delta_{\parallel} \bar{u} = 0. \end{cases}$$

330 The second equation forces \bar{u} to belong to the space \mathcal{G} of functions constant in the
 331 direction of anisotropy and the first equation defines the strong formulation of the
 332 limit problem (12) with \bar{q} acting as a Lagrange multiplier. \square

376 where σ and k are stabilization parameters chosen in order to match the scale of the
 377 scheme approximation error. Precisely, $k = 2$ for \mathbb{P}_1 -FEM and $k = 3$ for \mathbb{P}_2 -FEM. The
 378 difficulty here lies in the calibration of the stabilization parameters in order not to alter
 379 the precision of the scheme and to preserve a moderate condition number of the system
 380 matrix. The conditioning of the matrix for the discrete MMAP formulation depends
 381 on $1/h^4$ and $1/(\sigma h^{2+k})$ for the stabilized version [15]. It is therefore ε independent.

382 The method here introduced is well defined for all anisotropy topologies includ-
 383 ing closed field lines. The matrix stemming from the discretization of the operator
 384 Δ_{ε_0} is indeed invertible regardless of the anisotropy direction b . Moreover, the condi-
 385 tion number of the two scalar systems are not only ε independent, but it also scales
 386 more favorably, as $1/(\varepsilon_0 h^2)$, independently of the precision of the numerical method.
 387 The two field iterated method may appear similar to the stabilized MMAP scheme.
 388 However, at convergence this new formulation is completely equivalent to the original
 389 set of equations with no condition on ε_0 . This is a crucial feature that allows to
 390 choose ε_0 in a large range of values. Contrariwise, this choice is tightly constrained
 391 for the stabilization parameters and of course test case dependent. This new method
 392 hence permits to overcome the limitations of the stabilization methods for high order
 393 methods.

394 3. Numerical investigations.

395 **3.1. Introduction.** The goal of this section is to present some validation tests
 396 for the proposed method. We study the finite element formulation of the problem in
 397 different two dimensional settings, finite elements being usually a method of choice
 398 when dealing with elliptic problems. We consider two frameworks. The first one is
 399 a first order \mathbb{P}_1 -FEM on unstructured triangular grids. The second one relies on a
 400 Cartesian rectangular grid with a second order \mathbb{Q}_2 -FEM discretization.

401 Three configurations are considered:

- 402 1. A rectangular domain with open field lines and oscillating anisotropy direc-
 403 tions;
- 404 2. A ring shaped domain with closed circular field lines;
- 405 3. A rectangular domain with both open and closed lines.

406 The first test is performed with both \mathbb{P}_1 (unstructured grids) and \mathbb{Q}_2 (Cartesian Mesh)
 407 finite elements. The second test case is carried out with \mathbb{P}_1 -FEM and the last one
 408 with \mathbb{Q}_2 -FEM.

409 The iterative scheme presented herein relies on the iterative resolution of a mildly
 410 anisotropic problem for both u and q . The discretization of such problems by FEM
 411 may suffer from locking [3, 4]. We therefore propose to analyse how the locking effect
 412 can be circumvented thanks to the choice of the numerical method as well as the value
 413 of the parameter ε_0 . This later parameter defines the strength of the anisotropy in
 414 the problem solved at each step of the iterative process. It is thus a key point in
 415 parameterizing the efficiency of the numerical method.

416 Let us first focus on the finite element discretization of the iterative scheme.
 417 The finite element space \mathcal{V}_h denotes either the \mathbb{P}_1 or the \mathbb{Q}_2 elements defined on a
 418 discretization of the domain Ω with a mesh cell of typical size h . Let the homogeneous
 419 Dirichlet boundary conditions on Γ_D be enforced in the definition of \mathcal{V}_h , *i.e.* $\mathcal{V}_h \subset \mathcal{V}$.
 420 A discrete formulation of the scheme reads: find $(\bar{q}_h, \bar{u}_h) \in \mathcal{V}_h^2$, the stationary point

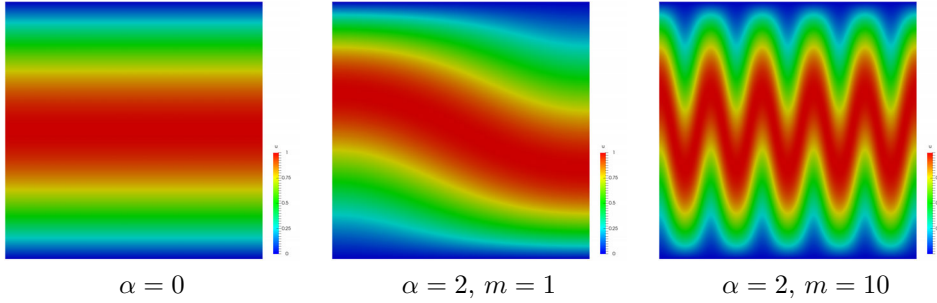


FIG. 1. *Test problem 1: Exact solution for three sets of parameters defining the anisotropy directions.*

of the sequence $(q_h^{n+1}, u_h^{n+1}) \in \mathcal{V}_h^2$, $n \geq 1$, solution to

$$(45) \quad \begin{cases} a_{\parallel}(u_h^{n+1}, v_h) + \varepsilon_0 a_{\perp}(u_h^{n+1}, v_h) = \varepsilon_0(f, v_h) - (\varepsilon_0 - \varepsilon)a_{\parallel}(q_h^n, v_h), & \forall v_h \in \mathcal{V}_h, \\ a_{\parallel}(q_h^{n+1}, w_h) + \varepsilon_0 a_{\perp}(q_h^{n+1}, w_h) = (f, w_h) - a_{\perp}(u_h^{n+1} - \varepsilon q_h^n, w_h), & \forall w_h \in \mathcal{V}_h, \end{cases}$$

In all the numerical investigations conducted in the sequel, the iterative method (45) is initiated with $q_h^0 = u_h^0 = 0$. The manufactured solution method is implemented in order to define the different setups. An analytic anisotropy direction is defined by means of a vector field b . The analytic expression of the problem solution u^ε is used together with that of b to compute the source term f accordingly to

$$f = -\Delta_{\perp} u^\varepsilon - \frac{1}{\varepsilon} \Delta_{\parallel} u^\varepsilon.$$

This expression is introduced in the system (45) to carry out the numerical approximation (\bar{q}_h, \bar{u}_h) . The component \bar{u}_h is thus compared against the exact analytic expression of the problem solution to evaluate the effectiveness of this new numerical method.

3.2. Test problem 1: Open field lines with oscillating anisotropy directions. Let $\Omega = [0, 1]^2$ be the square computational domain. Let us consider the anisotropy direction defined by

$$(46) \quad b = \frac{B}{|B|}, \quad B = \begin{pmatrix} \alpha(2y - 1) \cos(m\pi x) + \pi \\ \pi\alpha m(y^2 - y) \sin(m\pi x) \end{pmatrix},$$

where $m/2$ is the number of oscillation periods in the computational domain and α its amplitude. For $\alpha = 0$ this vector field is constant and aligned along the direction of x . When $\alpha > 0$ the field oscillates in the domain. The analytic solution of the problem is given by

$$(47) \quad u^\varepsilon = \sin(\pi y + \alpha(y^2 - y) \cos(m\pi x)) + \varepsilon \cos(2\pi x) \sin(\pi y),$$

Three configurations will be investigated. A constant anisotropy direction aligned the x -direction. This setup is defined by $\alpha = 0$. An anisotropy direction slowly varying in the computational domain, parametrized by $\alpha = 2$, $m = 1$. Finally an anisotropy direction with fast oscillations, defined by $\alpha = 2$, $m = 10$. For these computations, the anisotropy ratio is set to $\varepsilon = 10^{-15}$. Therefore the only variations of the problem

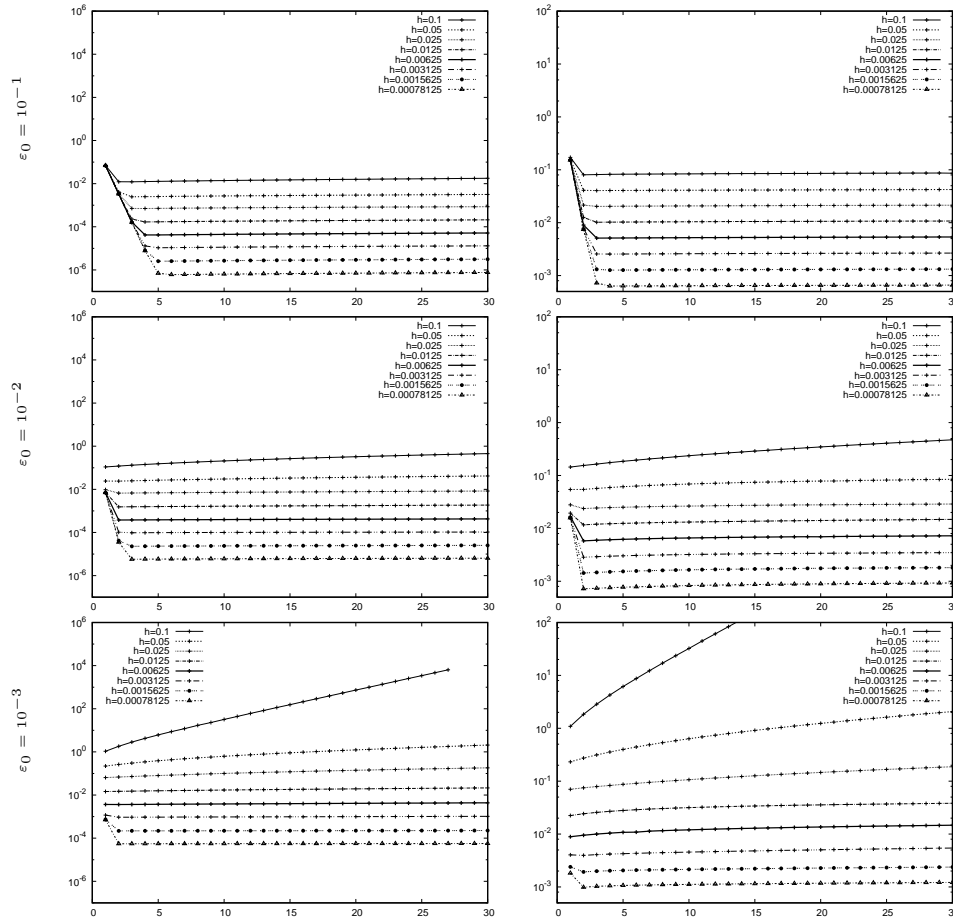


FIG. 2. Test Problem 1 (\mathbb{P}_1 -FEM, unstructured mesh): Relative L_2 (left) and H^1 (right) error as functions of the iteration number, for an anisotropy direction aligned with one coordinate ($\alpha = 0$) and different ε_0 -values.

450 solution occur along the direction defined by b . The plots displayed on Fig. 1 relate
 451 the solution as well as the anisotropy direction for the configurations precised above.

452 For these three anisotropies, the numerical method (45) is performed on 30 it-
 453 erations to define the numerical approximation \bar{u}_h carried out with different values
 454 for the parameter ε_0 , on eight different meshes with h ranging from $1/10$ to $1/1280$.
 455 The corresponding number of mesh vertices varies from 153 for the coarsest mesh to
 456 approximately $2 \cdot 10^6$ for the most refined mesh.

457 \mathbb{P}_1 -FEM, Unstructured triangular meshes.. The relative L_2 and H^1 errors are
 458 displayed on Figs. 2, 3 and 4 for the aligned, slowly and rapidly varying anisotropy
 459 directions defined above.

460 For the aligned anisotropy direction ($\alpha = 0$, see Fig. 2) and $\varepsilon_0 = 10^{-1}$ the
 461 convergence of the iterative method in the L_2 norm is obtained after at most five
 462 iterations (for the finest mesh) and after at most three iterations in the H^1 -norm.
 463 For $\varepsilon_0 = 10^{-2}$ the convergence is even faster with two iterations being sufficient for
 464 the H^1 -norm and three for the L_2 -norm. The results are however less precise than
 465 for $\varepsilon_0 = 10^{-1}$. Moreover, for the coarsest meshes the divergence of the iterations is

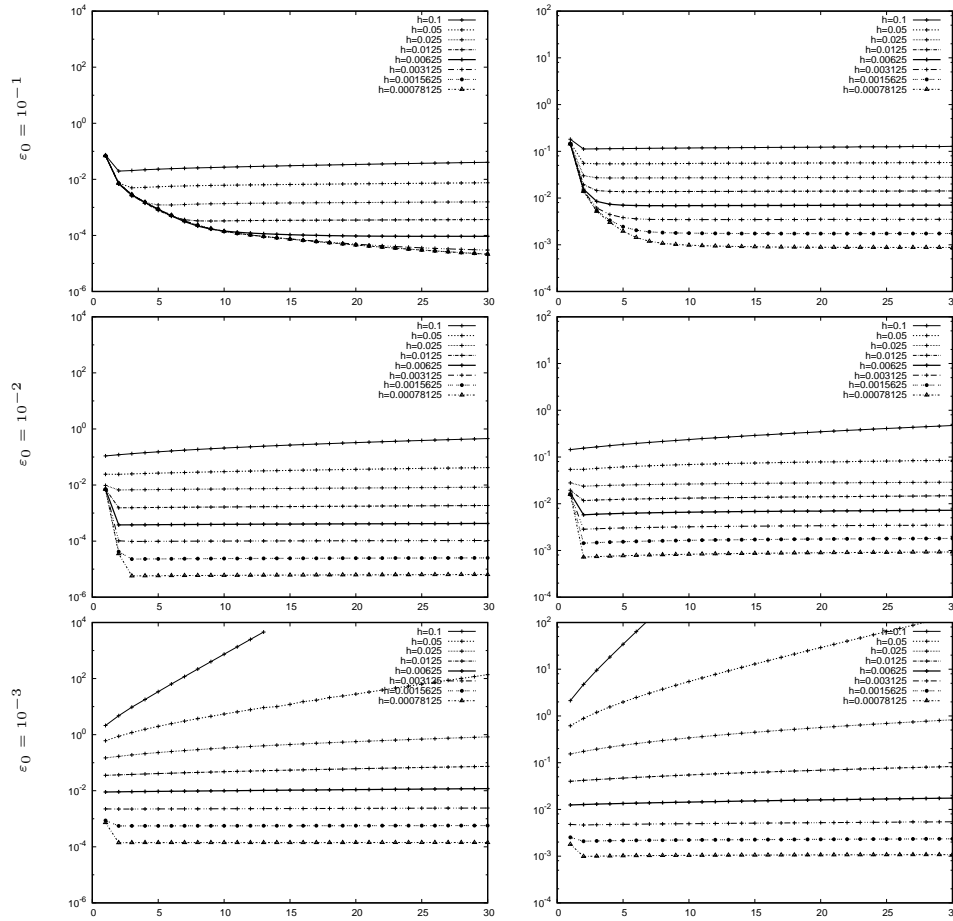


FIG. 3. Test Problem 1 (\mathbb{P}_1 -FEM, unstructured mesh): Relative L_2 (left) and H^1 (right) error as functions of the iteration number, for a slowly varying anisotropy direction ($\alpha = 2$, $m = 1$) and for different ε_0 -values.

466 observed. This is due to the locking phenomena, as explained in the next lines. This
 467 effect is even more visible with $\varepsilon_0 = 10^{-3}$.

468 For the slowly variable direction of anisotropy ($\alpha = 2$, $m = 1$, Fig. 3) the conver-
 469 gence is slow for $\varepsilon_0 = 10^{-1}$. The stationary point can not be reached in 30 iterations
 470 in the L_2 -norm for the most refined meshes. For intermediate and coarse meshes the
 471 convergence is however obtained in less than 10 iterations. The locking is causing slow
 472 divergence of the numerical solution for the coarsest mesh ($h = 10^{-1}$). For $\varepsilon_0 = 10^{-2}$
 473 the stationary point is reached in at most 3 iterations for both norms. Some locking
 474 effects are manifested in small augmentation of the error in course of the iterations.
 475 This is observed on the L_2 norm evolution for the coarsest mesh and for all meshes
 476 using the H^1 norm. For $\varepsilon_0 = 10^{-3}$ the stationary point is obtained in just two iter-
 477 ations for both norms. The precision is however worse compared to $\varepsilon_0 = 10^{-2}$ and
 478 the locking causes the relative error to blow up for two coarsest meshes. For these
 479 computations, the norm of the numerical solution is converging towards zero. This
 480 feature characterizes the locking.

481 In the most demanding test case with rapidly oscillating anisotropy direction

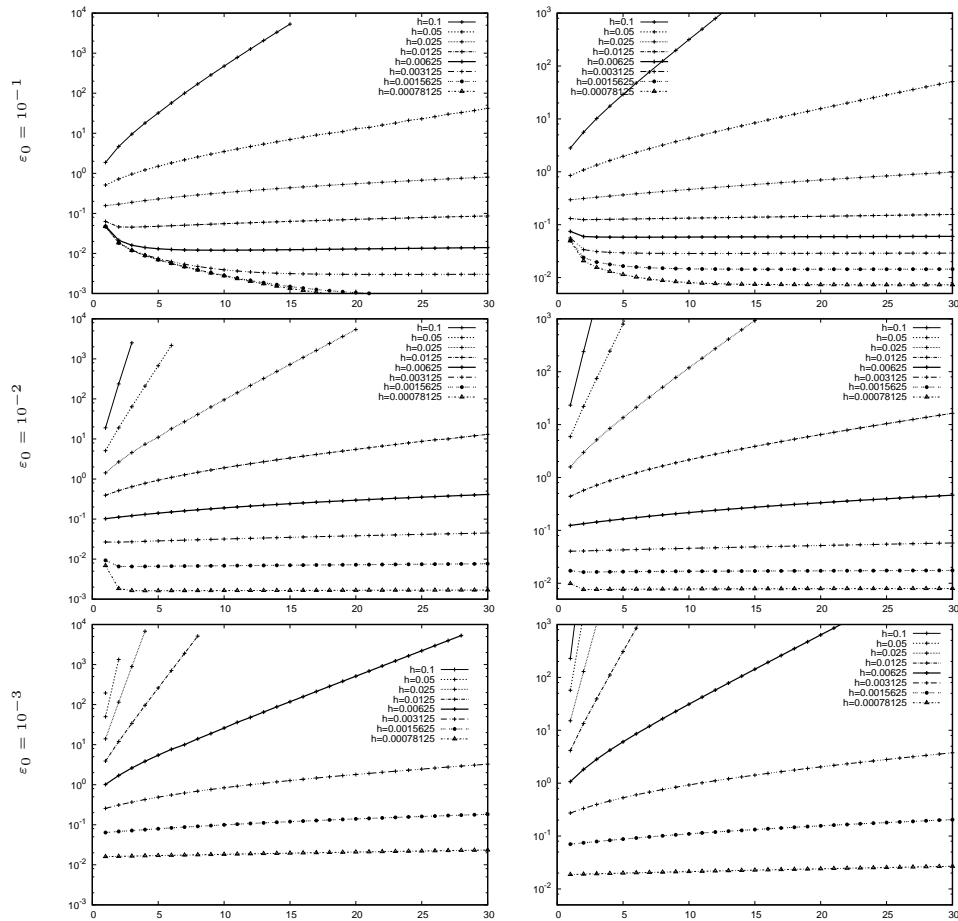


FIG. 4. Test Problem 1 (\mathbb{P}_1 -FEM, unstructured mesh): Relative L_2 (left) and H^1 (right) error as functions of the iteration number, for a rapidly varying anisotropy direction ($\alpha = 2$, $m = 10$) for different ε_0 -values.

482 ($\alpha = 2$, $m = 10$, Figure 4) the optimal value of ε_0 is again 10^{-2} : the stationary point
 483 is thus obtained after two iterations in both norms. The same convergence rate
 484 is obtained for $\varepsilon_0 = 10^{-3}$ but the numerical error is approximately ten times bigger
 485 with this setting. The locking allows accurate computations only on the finest meshes
 486 for this test case. For $\varepsilon_0 = 10^{-1}$ the convergence is very slow and the stationary point
 487 is not obtained for fine meshes in 30 iterations.

488 \mathbb{Q}_2 -FEM, Cartesian meshes.. The results related to these computations are gath-
 489 ered on Figs. 5–10. The use of Cartesian grids eliminates the locking phenomenon
 490 for the anisotropy aligned with one coordinate (see Figs 5 and 6 related to $\alpha = 0$).
 491 The stationary point is reached in 8 iterations for $\varepsilon_0 = 10^{-1}$, in 4 for $\varepsilon_0 = 10^{-2}$, 3
 492 for $\varepsilon_0 = 10^{-3}$ and 2 for $\varepsilon_0 = 10^{-4}$. The precision remains the same whatever the
 493 values of ε_0 for the H^1 norm (see Fig. 6). An increase of the L_2 error norm is ob-
 494 served for the most refined meshes and the smallest ε_0 -value (10^{-4}). One can indeed
 495 observe on Fig. 5 that the L_2 error increases when the number of cells ranges from
 496 320×320 ($h = 0.003125$) to 640×640 ($h = 0.0015625$) and then to 1280×1280
 497 ($h = 0.00078125$). Similar conclusions hold true for the computations carried out on

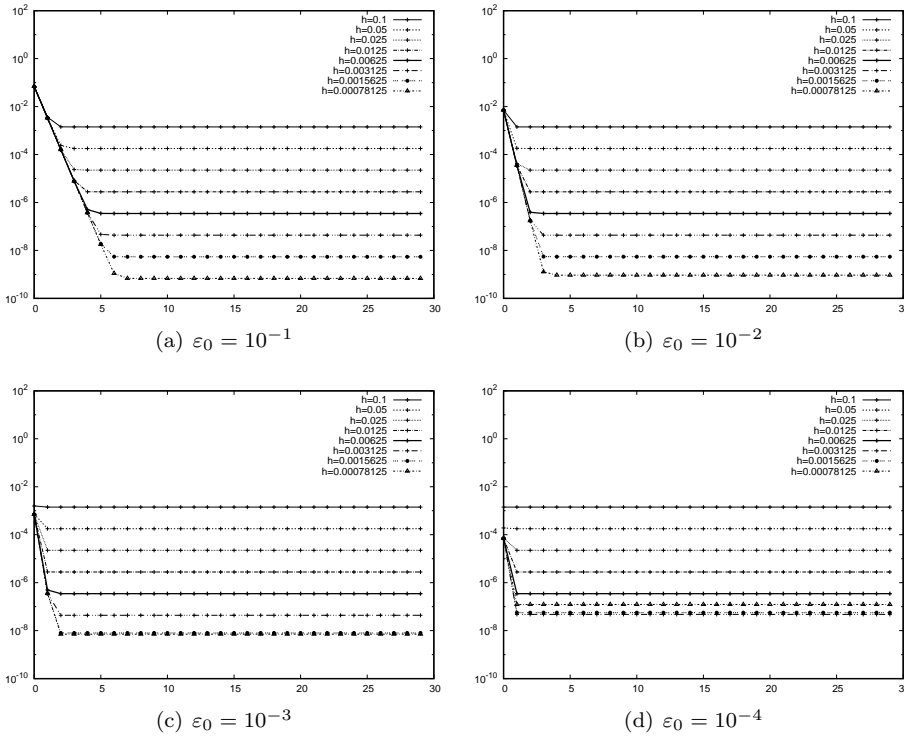


FIG. 5. Test Problem 1 (\mathbb{Q}_2 -FEM, Cartesian grid): Relative L_2 error as a function of the iteration number for an anisotropy direction aligned with one coordinate ($\alpha = 0$) and for different ε_0 -values.

498 the two most refined meshes with $\varepsilon_0 = 10^{-3}$.

499 This loss of precision is explained by the conditioning of the matrix (stemming
500 from the discretization of the operator Δ_{ε_0}), which is proportional to $1/\varepsilon_0 h^2$. For the
501 most refined meshes and the smallest values of ε_0 , the condition number of this matrix
502 (computed by MUMPS [1, 2]) is estimated as large as 10^9 . Therefore computing a
503 numerical approximation with a precision larger than 10^{-6} is out of reach. The
504 condition number estimated for $\varepsilon_0 = 10^{-1}$ is of the order of 10^6 which accounts for
505 the improved precision (10^{-9}) obtained with this value of the parameter.

506 For the varying anisotropy directions the second order finite elements help to
507 prevent the locking. This is a feature documented in the literature [3, 4]. For the
508 slowly varying case (Figs 7 and 8) the numerical solution converges even for the coarse
509 meshes except for the smallest value $\varepsilon_0 = 10^{-4}$. However, even in this case, no blow
510 up of the error is observed. For $\varepsilon_0 = 10^{-1}$ the stationary point is reached in up to 12
511 iterations for mesh sizes smaller than or equal to 80×80 ($h \leq 0.025$) for the L_2 norm.
512 For finer meshes the algorithm does not converge within 30 iterations in the L_2 norm
513 (Fig. 7). In the H^1 norm (see Fig. 8) the convergence is obtained for mesh sizes smaller
514 than or equal to 320×320 ($h \leq 0.003125$). The best performance for intermediate and
515 refined meshes is obtained for ε_0 -values in the range $[10^{-4}, 10^{-3}]$. The convergence
516 is thus obtained after three iterations only. For coarse meshes however some locking
517 effects are still observed with the deterioration of the precision, more apparent for the
518 smallest ε_0 -values.

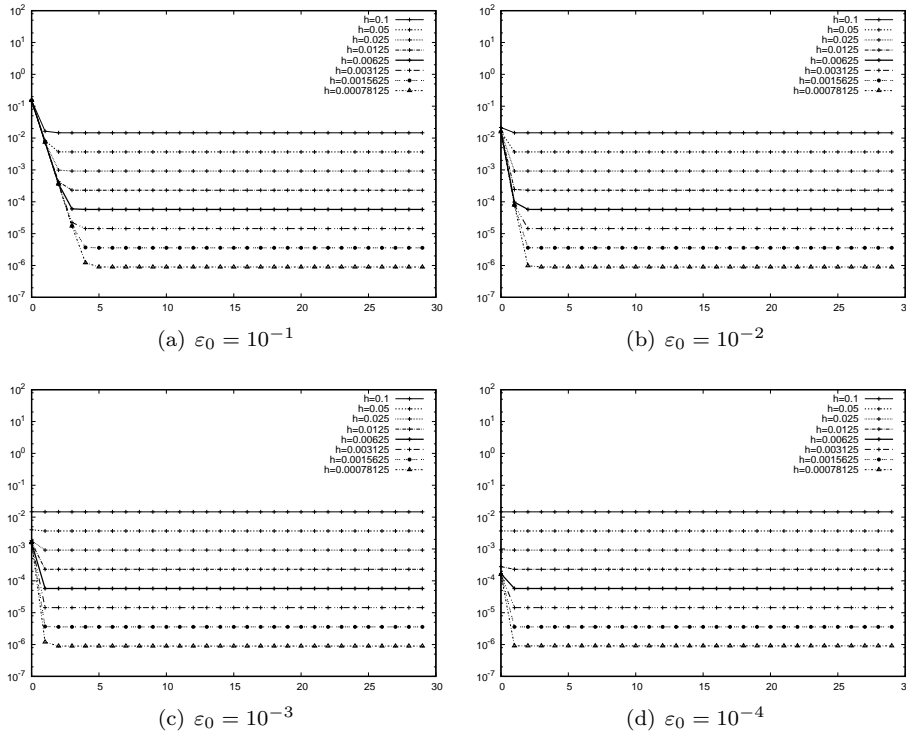


FIG. 6. Test Problem 1 (\mathbb{Q}_2 -FEM, Cartesian grid): Relative H^1 error as a function of the iteration number for an anisotropy direction aligned with one coordinate ($\alpha = 0$) and for different ε_0 -values.

519 When the anisotropy direction is varying rapidly in the computational domain
 520 (Figures 9 and 10), the locking is causing the blow up of the numerical error for coarse
 521 meshes. Here also, the norm of the numerical approximation is observed to converge
 522 towards zero. For intermediate and refined meshes, the convergence is observed for
 523 all values of ε_0 . The convergence rate increases with the vanishing of ε_0 . The best
 524 numerical precision is obtained for $\varepsilon_0 = 10^{-3}$.

525 *Partial conclusions and comments.* This first test case is intended to asses the
 526 importance of the parameter ε_0 and the robustness of the method with respect to the
 527 choice of its value.

528 The convergence rate of the iterative method increases with the diminishing of
 529 ε_0 . However the values of this parameter have to be kept large enough to prevent
 530 the locking as well as the deterioration of the matrix condition number. The locking
 531 alters the convergence of the method for the coarsest meshes. The deterioration of the
 532 matrix conditioning is more detrimental for the most refined meshes. It prevents to
 533 obtain the optimal precision from the numerical method. The comparisons of the first
 534 and second order methods demonstrate that the locking effect can be avoided thanks
 535 to the use of high order discretizations. Indeed the locking is almost removed when
 536 \mathbb{Q}_2 finite element discretizations are used. It only remains for the coarsest meshes.
 537 However this weakness should be put into perspective. Indeed coarse meshes do not
 538 contain enough points to resolve accurately the variations of the anisotropy. Hence
 539 any numerical method can hardly yield acceptable results. With high order methods

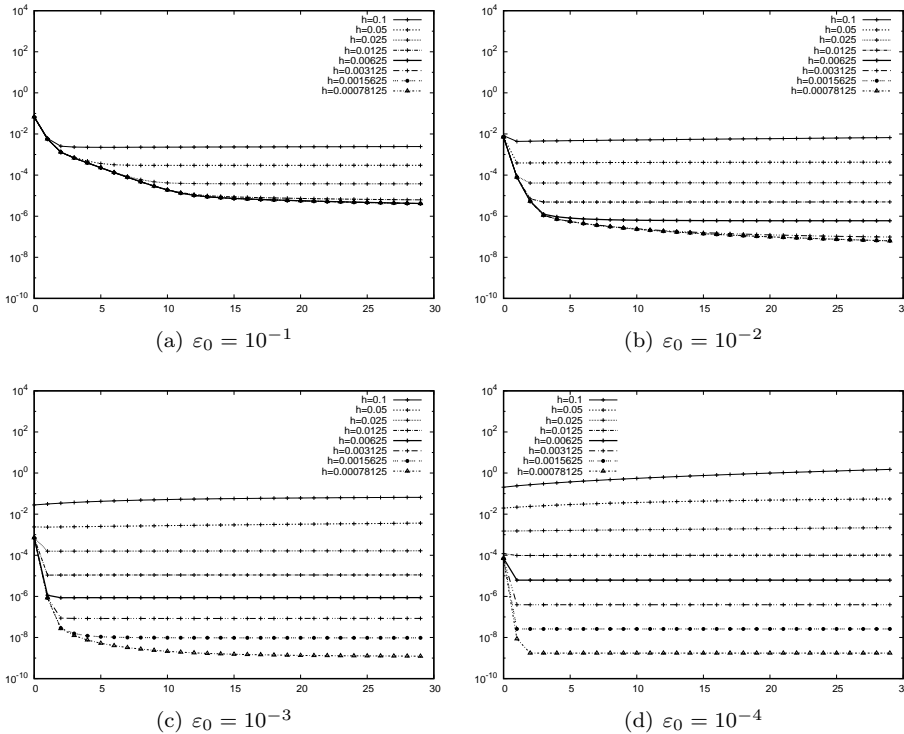


FIG. 7. Test Problem 1 (\mathbb{Q}_2 -FEM, Cartesian grid): Relative L_2 error for a slowly varying anisotropy direction ($\alpha = 2$, $m = 1$) and different ε_0 -values.

540 (\mathbb{Q}_2 -FEM), the iterative method introduced in this paper is robust with respect to
 541 the choice of the parameter ε_0 . The convergence is secured for the values of this
 542 parameter between 10^{-3} and 10^{-2} for all the computations carried out in the frame
 543 of this first test case. With $\varepsilon_0 = 10^{-4}$ the convergence is obtained in less than 10
 544 iterations for all the investigations conducted. To be complete, it should be pointed
 545 out that the maximum performance of the method may be obtained with test case
 546 specific value (2 to 5 iterations).

547 Note that the results reported in the precedent figures are related to computations
 548 carrying out anisotropy strength as large as 10^{15} . No significant differences have been
 549 observed over the range of ε -values in $[10^{-20}, 10^{-6}]$ regarding the method precision,
 550 convergence properties and optimal choice of the parameter ε_0 .

551 *Comparisons with MMAP scheme..* The MMAP scheme, introduced in [11], con-
 552 sists in solving the two fields (u, q) problem (42). In this system, the uniqueness of
 553 the auxiliary variable q is provided by demanding additionally that $q = 0$ on the part
 554 of the boundary where the field lines enter the computational domain ($b \cdot n > 0$).

555 A comparison of the precision of the two field iterative method and the MMAP
 556 method is reported in Tab. 1. Note that the conditioning of the matrix associated with
 557 the MMAP scheme is proportional to $1/h^4$. It is estimated as large as 10^{12} for the
 558 aligned ($\alpha = 0$) and rapidly varying anisotropy directions ($\alpha = 2, m = 10$) and 10^{10}
 559 for slowly varying directions ($\alpha = 2, m = 1$) for the most refined mesh considered
 560 so far (1280×1280 , $h = 0.00078125$). The large matrix conditioning deteriorates
 561 the precision of the method for the aligned case for the finest mesh and the optimal

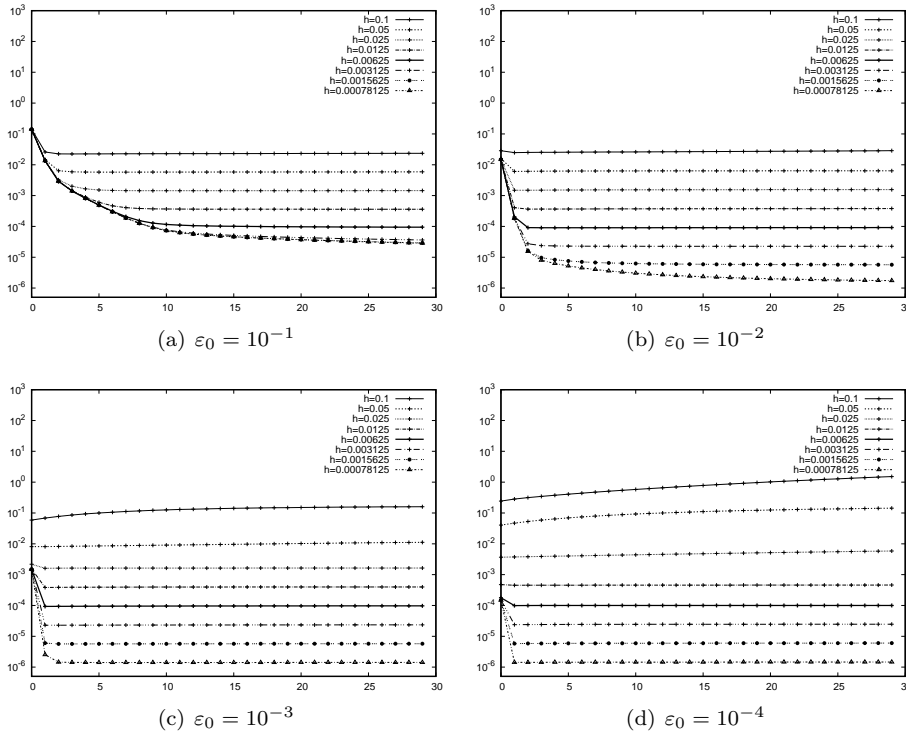


FIG. 8. Test Problem 1 (\mathbb{Q}_2 -FEM, Cartesian grid): Relative H^1 error for a slowly varying anisotropy direction ($\alpha = 2$, $m = 1$) and different ε_0 -values.

method	$\alpha = 0$				$\alpha = 2, m = 1$				$\alpha = 2, m = 10$			
	L_2	#	H^1	#	L_2	#	H^1	#	L_2	#	H^1	#
MMA	$9.68 \cdot 10^{-8}$		$8.52 \cdot 10^{-5}$		$1.47 \cdot 10^{-9}$		$1.46 \cdot 10^{-6}$		$4.31 \cdot 10^{-7}$		$1.36 \cdot 10^{-4}$	
$\varepsilon_0 = 10^{-1}$	$6.85 \cdot 10^{-10}$	8	$8.98 \cdot 10^{-7}$	6	$4.11 \cdot 10^{-6}$	-	$2.86 \cdot 10^{-5}$	-	$1.72 \cdot 10^{-3}$	-	$4.84 \cdot 10^{-3}$	-
$\varepsilon_0 = 10^{-2}$	$9.36 \cdot 10^{-10}$	5	$8.98 \cdot 10^{-7}$	3	$6.28 \cdot 10^{-8}$	-	$1.74 \cdot 10^{-6}$	-	$1.19 \cdot 10^{-5}$	-	$1.52 \cdot 10^{-4}$	-
$\varepsilon_0 = 10^{-3}$	$7.11 \cdot 10^{-9}$	3	$8.98 \cdot 10^{-7}$	3	$1.23 \cdot 10^{-9}$	12	$1.42 \cdot 10^{-6}$	4	$1.81 \cdot 10^{-6}$	5	$1.36 \cdot 10^{-4}$	3
$\varepsilon_0 = 10^{-4}$	$1.23 \cdot 10^{-7}$	2	$9.07 \cdot 10^{-7}$	2	$1.74 \cdot 10^{-9}$	3	$1.43 \cdot 10^{-6}$	2	$1.78 \cdot 10^{-5}$	2	$1.38 \cdot 10^{-4}$	2

TABLE 1

Test Problem 1: Comparisons of the precision of the MMA and the iterative method for a \mathbb{Q}_2 -FEM discretization on a mesh with 1280×1280 points ($h = 0.00078125$). The number of iterations required to obtain the smallest relative error in L_2 and H^1 norms is reported for the different ε_0 -values parameterizing the iterative method (“-” meaning that the method has not converged in 30 iterations).

562 convergence rate is lost. That explains the fact that the iterative scheme is 100 more
563 precise than the MMA method in this configuration. For less refined meshes, the
564 MMA scheme and the iterative scheme with $\varepsilon_0 \sim 10^{-3}$ yield similar precision.

565 The numerical efficiency of the two methods are now compared. It may seem at
566 first glance that the iterative scheme is more time consuming than the MMA method
567 as it requires several resolutions of a linear system. However, the system related to
568 the iterative scheme is twice as small and hence its resolution is faster and requires
569 less memory in comparison to the MMA scheme. Moreover the iteration number
570 to convergence is small when ε_0 is close to the optimal range of values. In Tab. 2 a
571 comparison of the computational time for both methods is proposed. The same sparse

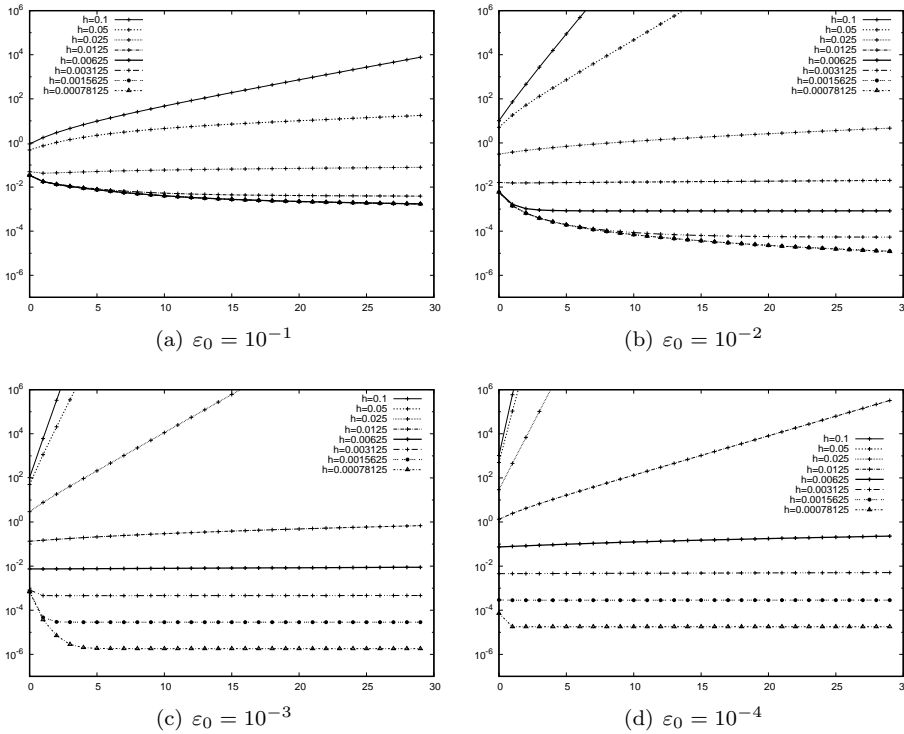


FIG. 9. *Test Problem 1 (\mathbb{Q}_2 -FEM, Cartesian grid): Relative L_2 error for a rapidly varying anisotropy direction ($\alpha = 2$, $m = 10$) and different ε_0 -values.*

572 direct solver, namely the MUMPS package [1, 2] is used to implement the LU matrix
 573 factorization and solve the linear systems involved in any method. These results show
 574 that the MMAP method is approximately twice as fast on coarse and intermediate
 575 meshes. On the 640×640 mesh it is the iterative scheme that performs better. Finally,
 576 for the finest mesh (1280×1280), the difference is clearly in favour of the iterative
 577 scheme which turns to be seven times faster. The computational cost required for the
 578 resolution of a linear system twice as large explains the poor efficiency of the MMAP
 579 compared to the iterative method for the largest mesh. Solving few times a linear
 580 system with a small size is more efficient than solving once a large linear system.

581 **3.3. Test problem 2 — diffusion in a ring.** This test case reproduces the
 582 framework proposed in [7] and [17] investigating anisotropic diffusion problems in a
 583 Torus. It consists in simulating the diffusion in a circular domain, a context repre-
 584 sentative of magnetized plasma simulation for Tokamaks. The computational domain
 585 is defined by $\Omega = \{(x, y) \in \mathbb{R}^2 | 0.25 \leq x^2 + y^2 \leq 1\}$ and the anisotropy direction is
 586 given by the field b provided in polar coordinates (r, θ) :

$$587 \quad (48) \quad b = \begin{pmatrix} \cos \theta \\ -\sin \theta \end{pmatrix} .$$

589 The analytic solution of the original problem, as represented on Fig. 11, is given by

$$590 \quad (49) \quad u^\varepsilon = -\sin(2\pi r) + \varepsilon \sin(2\pi r) \cos \theta .$$

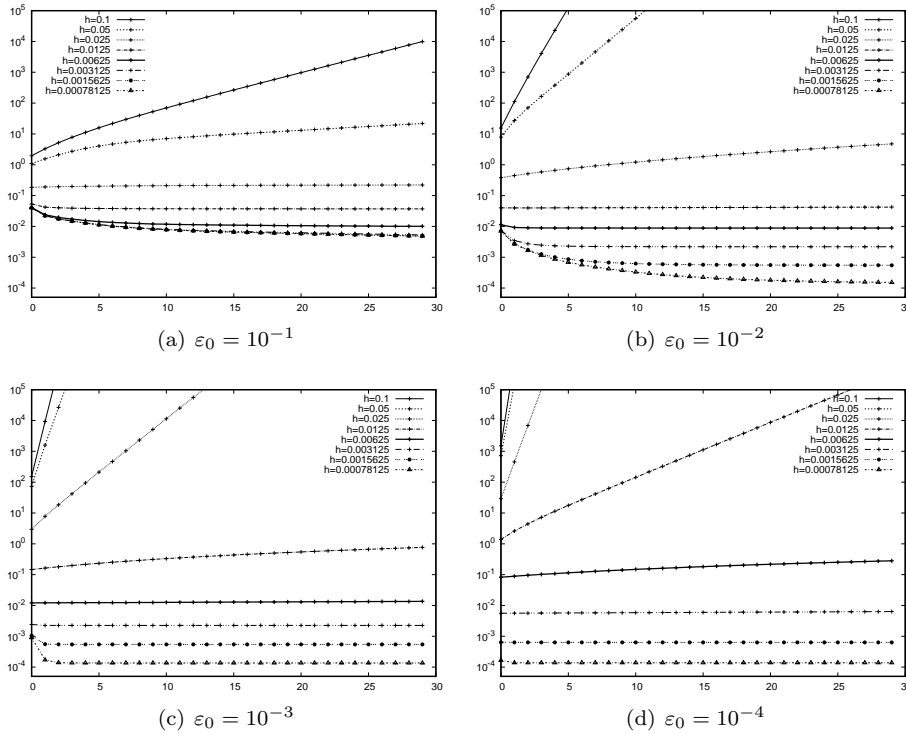


FIG. 10. Test Problem 1 (\mathbb{Q}_2 -FEM, Cartesian grid): Relative H^1 error for a rapidly varying anisotropy direction ($\alpha = 2$, $m = 10$) and different ε_0 -values.

Mesh	iterative scheme				MMAP
	total	per iter.	iter. to conv.	time to conv.	
10^2	0.181s	0.006s	2	0.012s	0.009s
20^2	0.477s	0.016s	2	0.032s	0.018s
40^2	1.992s	0.066s	2	0.132s	0.063s
80^2	8.051s	0.268s	2	0.536s	0.282s
160^2	36.07s	1.202s	2	2.404s	1.121s
320^2	144s	4.8s	2	9.6s	5.5s
640^2	9m42s	19.4s	3	58.2s	1m42s
1280^2	44m16s	1m28s	5	7m20s	52m28s

TABLE 2

Comparison of the runtime of the iterative scheme (total runtime for 30 iterations, time per iteration, number of iterations for convergence and time to convergence) with the runtime obtained for the MMAP scheme for \mathbb{Q}_2 -FEM on different mesh. Runtimes obtained on the MacBook Pro laptop equipped with a 3.1 GHz Intel Core i7 dual core processor, 16GB of RAM and a Solid State Drive. The code is written in fortran compiled with gfortran-5.4.0 with `-Ofast -march=corei7` optimization flags.

592 These simulations are only performed on unstructured meshes (triangles and \mathbb{P}_1 -
593 FEM) with $\varepsilon = 10^{-15}$ defining a severe anisotropy. It is important to notice, that
594 standard discretization of this problem, although much more elaborated than the one
595 implemented herein (see for instance [7, 17, 18]) cannot handle anisotropy strengthes
596 ε^{-1} larger than $\sim 10^4$, this ratio being limited to 10^{-2} in [7, 18]. It is important also

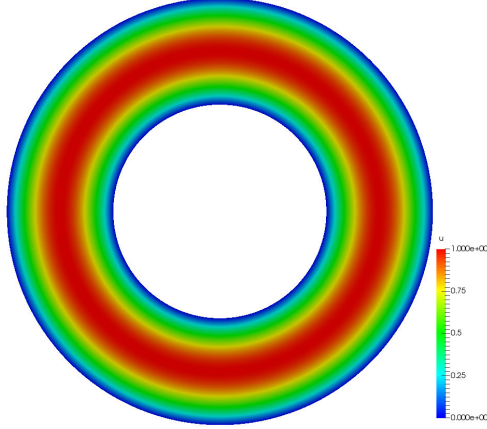


FIG. 11. *Exact solution for the test problem 2.*

597 to point out that the elliptic problem addressed in the present paper is much more
 598 demanding, from the numerical point of view, than the diffusion problem considered
 599 by other authors. Indeed the discretization of the time derivative of the solution intro-
 600 duces a mass matrix offsetting partially the anisotropy. This effect is more significant
 601 than the time step values are small. This artefact is not present in the system at
 602 hand in the present work, addressing the stationary problem. This guarantees that
 603 the numerical parameters can be set accordingly to the physics of interest rather than
 604 to prevent the deterioration of the matrix conditioning. The convergence results of
 605 the two field iterated method are presented in Fig. 12.

606 The scheme behaves well for this test case too. The conclusions drawn from the
 607 preceding investigations hold true for this setup. The solution converges rapidly to
 608 the stationary point for $\varepsilon_0 = 10^{-2}$ and $\varepsilon_0 = 10^{-3}$. For $\varepsilon_0 = 10^{-1}$ the convergence is
 609 very slow and the stationary point is attained for the coarsest meshes only. The best
 610 precision is obtained for $\varepsilon_0 = 10^{-2}$.

611 **3.4. Test problem 3 — magnetic islands.** The last test case is also related to
 612 the physics describing hot plasmas in Tokamaks. The main difficulty of this test case
 613 is the presence of two so-called magnetic islands. They consist of closed magnetic field
 614 lines in some specific regions of the domain. Some of the magnetic field lines are open
 615 and reconnect the boundaries of the domain, the other being closed. In the sequel, the
 616 typical size of these structures will be parametrized by a (in our simulations $a = 0.05$).
 617 The computational domain is square $\Omega = [0, 1]^2$. If B represents the local magnetic
 618 field, $b = B/|B|$ is the vector field defining the direction of anisotropy with

$$619 \quad (50) \quad b = \frac{B}{|B|}, \quad B = \begin{pmatrix} -\cos(\pi y) \\ 4a \sin(4\pi x) \end{pmatrix}.$$

621 The analytical solution is either given by

$$622 \quad (51) \quad u^\varepsilon = \sin(\sin(\pi y) - a \cos(4\pi x)) + \varepsilon \cos(2\pi x) \sin(2\pi y),$$

624 or

$$625 \quad (52) \quad u^\varepsilon = \sin(10(\sin(\pi y) - a \cos(4\pi x))) + \varepsilon \cos(2\pi x) \sin(10\pi y).$$

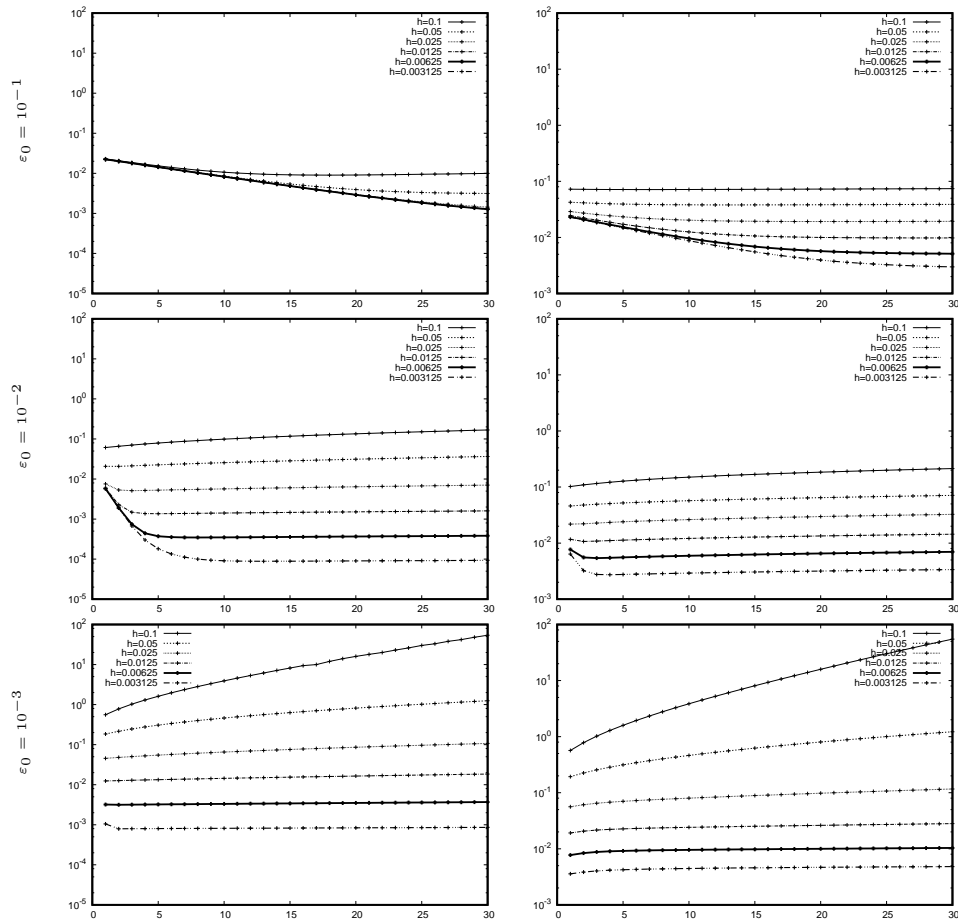


FIG. 12. Test problem 2: Relative L_2 (left) and H^1 (right) error norms for different values of ε_0 and a \mathbb{P}_1 -FEM on different mesh resolutions.

627 The first solution is mildly oscillating in the domain and while the second defines a
 628 highly oscillatory solution, which is challenging for a numerical method to capture.
 629 The analytical solutions as well as the anisotropy direction are presented on Fig. 13.

630 The source term of the problem is analytically computed according to the preceding
 631 definitions of the anisotropy direction and solutions, in order to implement the
 632 manufactured solution technique.

633 The numerical convergence of the iterative scheme for intermediate and refined
 634 meshes and values of ε_0 equal to 10^{-3} and 10^{-4} is presented in Figs. 14 and 15. With
 635 the largest value of ε_0 the convergence is very slow and for coarse meshes the locking
 636 prevents the convergence. Even on fine meshes the scheme has not converged in 30
 637 iterations in both slowly and rapidly oscillating variants. We did not observe any
 638 significant difference in the convergence speed for both setups. For the smallest value
 639 of ε_0 the convergence is observed except for the two coarsest meshes.

640 **4. Conclusions.** In this paper a new Asymptotic-Preserving scheme is intro-
 641 duced for the efficient resolution of anisotropic elliptic equations. This method con-
 642 sists in iterating the resolution of two one field problems which require the solution

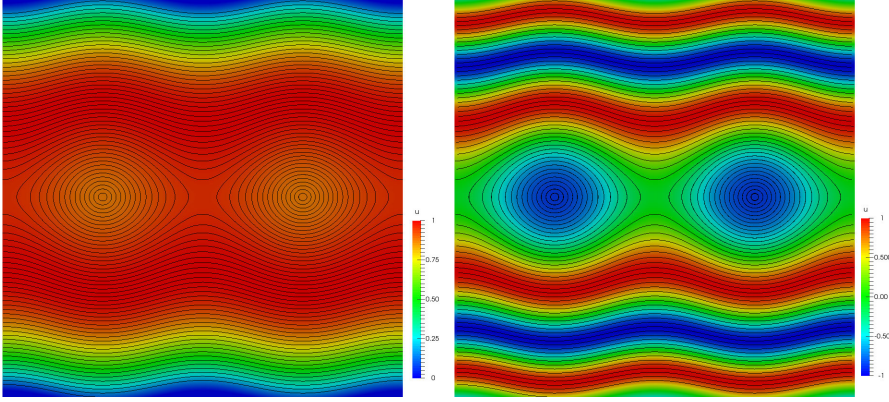


FIG. 13. Test problem 3: Exact solutions as defined by Eqs. (51) (left) and (52) (right) and anisotropy direction.

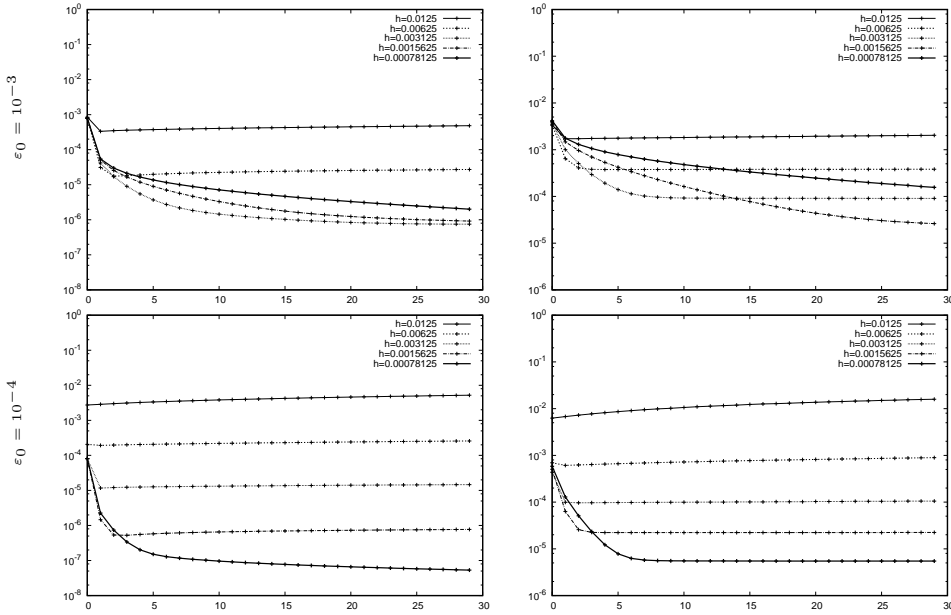


FIG. 14. Test problem 3: Relative L_2 (left) and H^1 (right) errors as functions of the number of iterations for the slowly oscillating solution carried out with a \mathbb{Q}_2 -FEM on several meshes and different values of ε_0 .

643 of the same linear system. This system is issued from the discretization of a mildly
 644 anisotropic problem, parameterized by a numerical parameter $\varepsilon_0 \gg \varepsilon$, where ε^{-1} is
 645 the strength of the anisotropy. The advantages of this new scheme are three fold. First
 646 the method can address any topology of anisotropies including closed field lines. Sec-
 647 ond, the condition number of the linear systems solved for the iterated method scales
 648 better than that of other asymptotic-preserving (Micro-Macro) methods. Third, the
 649 computational efficiency of the method may be substantially improved with respect
 650 to these same methods. This is already demonstrated for large meshes in two dimen-
 651 sional frameworks. More substantial gains can be anticipated for three dimensional

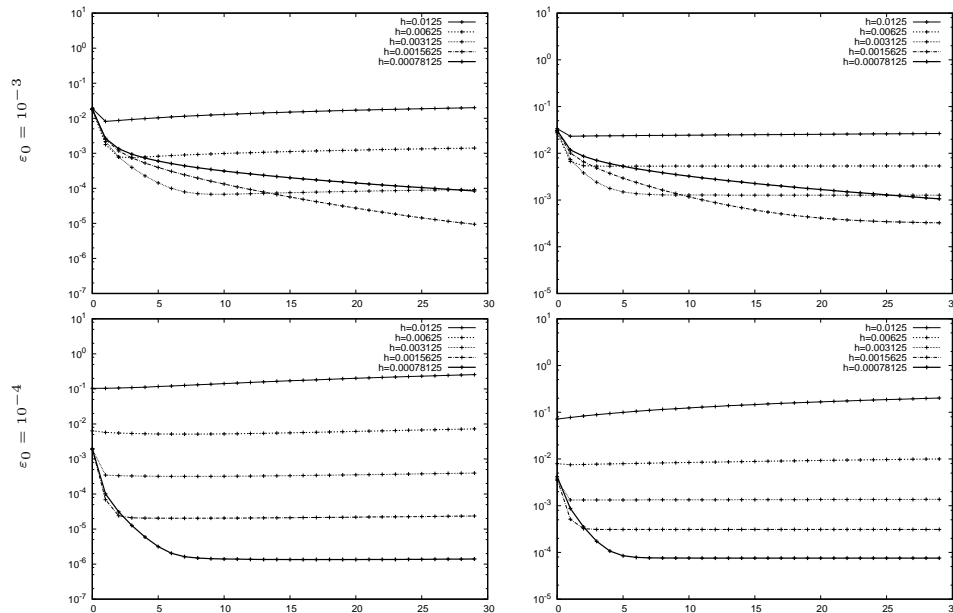


FIG. 15. Test problem 3: Relative L_2 (left) and H^1 (right) errors as functions of the number of iterations for the rapidly oscillating solution carried out with a \mathbb{Q}_2 -FEM on several meshes and different values of ε_0 .

652 computations since the linear systems at hand are issued from classical elliptic prob-
653 lems for which very efficient solvers can be used. This issue will be investigated in
654 subsequent works. The method already appears to be robust with respect to the
655 choice of ε_0 and do not suffer from the locking effect provided that high order meth-
656 ods and refined meshes are used. The convergence of the iterations is improved for
657 small ε_0 -values, however at the price of a deterioration of the matrix conditioning.
658 Future works will also be devoted to the construction of preconditioners, in order to
659 offset the deterioration of the matrix conditioning when increasing the anisotropy of
660 the inner problems.

661 **Acknowledgements.** This work has been carried out within the framework of
662 the EUROfusion Consortium and has received funding from the Euratom research
663 and training programme 2014-2018 under grant agreement No 633053. The views
664 and opinions expressed herein do not necessarily reflect those of the European Com-
665 mission.

666 This work has been supported by the french “Agence Nationale pour la Recherche
667 (ANR)” in the frame of the contract ANR-11-MONU-009-01 “MOONRISE: MOD-
668 els, Oscillations and NumeRical SchEmes” (2015-2019) as well as the “labex CIMI”
669 (International Centre for Mathematics and Computer Science in Toulouse) in the
670 frame of the project “SCANISO: SCalable solvers for ANISOtropic equations arising
671 in magnetized plasma simulations” (2017-2019). Support from the “Fédération de
672 Fusion pour la Recherche par Confinement Magnétique” (FrFCM) in the frame of
673 the project AAPFR17_2TTB “APREMADAD: Asymptotic-PREserving methods for
674 MAGnetized Plasma simulations : Drift fluid limit and Anisotropic Diffusion prob-
675 lems” (2017-2018) is also acknowledged.

- 677 [1] P. R. AMESTOY, I. S. DUFF, J.-Y. L'EXCELLENT, AND J. KOSTER, *A Fully Asynchronous Mul-*
678 *tifrontal Solver Using Distributed Dynamic Scheduling*, SIAM Journal on Matrix Analy-
679 *sis and Applications*, 23 (2001), pp. 15–41, <https://doi.org/10.1137/S0895479899358194>,
680 <http://epubs.siam.org/doi/abs/10.1137/S0895479899358194> (accessed 2013-11-21).
- 681 [2] P. R. AMESTOY, A. GUERMOUCHE, AND S. PRALET, *Hybrid scheduling for the parallel solution*
682 *of linear systems*, Parallel Computing, 32 (2006), pp. 136–156.
- 683 [3] I. BABUŠKA AND M. SURI, *Locking effects in the finite element approximation of elas-*
684 *ticity problems*, Numerische Mathematik, 62 (1992), pp. 439–463, [https://doi.org/10.](https://doi.org/10.1007/BF01396238)
685 [1007/BF01396238](https://doi.org/10.1007/BF01396238), <https://link.springer.com/article/10.1007/BF01396238> (accessed 2017-
686 08-05).
- 687 [4] I. BABUŠKA AND M. SURI, *On Locking and Robustness in the Finite Element Method*,
688 SIAM Journal on Numerical Analysis, 29 (1992), pp. 1261–1293, [https://doi.org/10.1137/](https://doi.org/10.1137/0729075)
689 [0729075](https://doi.org/10.1137/0729075), <http://epubs.siam.org/doi/abs/10.1137/0729075> (accessed 2017-08-05).
- 690 [5] C. BESSE, F. DELUZET, C. NEGULESCU, AND C. YANG, *Efficient numerical methods for strongly*
691 *anisotropic elliptic equations*, J Sci Comput, 55 (2013), pp. 231–254, [https://doi.org/10.](https://doi.org/10.1007/s10915-012-9630-7)
692 [1007/s10915-012-9630-7](https://doi.org/10.1007/s10915-012-9630-7), <http://link.springer.com/article/10.1007/s10915-012-9630-7> (ac-
693 cessed 2013-08-19).
- 694 [6] L. CHACÓN, D. DEL CASTILLO-NEGRETE, AND C. D. HAUCK, *An asymptotic-preserving semi-*
695 *lagrangian algorithm for the time-dependent anisotropic heat transport equation*, Journal
696 of Computational Physics, 272 (2014), pp. 719–746, [https://doi.org/10.1016/j.jcp.2014.](https://doi.org/10.1016/j.jcp.2014.04.049)
697 [04.049](https://doi.org/10.1016/j.jcp.2014.04.049), <http://www.sciencedirect.com/science/article/pii/S0021999114003258> (accessed
698 2014-08-19).
- 699 [7] N. CROUSEILLES, M. KUHN, AND G. LATU, *Comparison of Numerical Solvers for Anisotropic*
700 *Diffusion Equations Arising in Plasma Physics*, Journal of Scientific Computing, (2015),
701 pp. 1–38, <https://doi.org/10.1007/s10915-015-9999-1>, [http://link.springer.com/article/10.](http://link.springer.com/article/10.1007/s10915-015-9999-1)
702 [1007/s10915-015-9999-1](http://link.springer.com/article/10.1007/s10915-015-9999-1) (accessed 2015-10-12).
- 703 [8] P. DEGOND, *Asymptotic-preserving schemes for fluid models of plasmas*, Panoramas et
704 *synthèses of the SMF*, 39-40 (2013), pp. 1–90, <http://arxiv.org/abs/1104.1869> (accessed
705 2012-04-17).
- 706 [9] P. DEGOND AND F. DELUZET, *Asymptotic-Preserving methods and multiscale models*
707 *for plasma physics*, Journal of Computational Physics, 336 (2017), pp. 429–457,
708 <https://doi.org/10.1016/j.jcp.2017.02.009>, [http://www.sciencedirect.com/science/article/](http://www.sciencedirect.com/science/article/pii/S002199911730102X)
709 [pii/S002199911730102X](http://www.sciencedirect.com/science/article/pii/S002199911730102X) (accessed 2017-03-16).
- 710 [10] P. DEGOND, F. DELUZET, A. LOZINSKI, J. NARSKI, AND C. NEGULESCU, *Duality-based*
711 *asymptotic-preserving method for highly anisotropic diffusion equations*, Communications
712 in Mathematical Sciences, 10 (2012), pp. 1–31, [https://doi.org/10.4310/CMS.2012.v10.](https://doi.org/10.4310/CMS.2012.v10.n1.a2)
713 [n1.a2](https://doi.org/10.4310/CMS.2012.v10.n1.a2), [http://www.intlpress.com/site/pub/pages/journals/items/cms/content/vols/0010/](http://www.intlpress.com/site/pub/pages/journals/items/cms/content/vols/0010/0001/a002/)
714 [0001/a002/](http://www.intlpress.com/site/pub/pages/journals/items/cms/content/vols/0010/0001/a002/) (accessed 2015-10-01).
- 715 [11] P. DEGOND, A. LOZINSKI, J. NARSKI, AND C. NEGULESCU, *An asymptotic-preserving method*
716 *for highly anisotropic elliptic equations based on a micro-macro decomposition*, Journal
717 of Computational Physics, 231 (2012), pp. 2724–2740, [https://doi.org/10.1016/j.jcp.2011.](https://doi.org/10.1016/j.jcp.2011.11.040)
718 [11.040](https://doi.org/10.1016/j.jcp.2011.11.040), <http://www.sciencedirect.com/science/article/pii/S0021999111006966> (accessed
719 2012-04-17).
- 720 [12] S. GÜNTER, K. LACKNER, AND C. TICHMANN, *Finite element and higher order difference*
721 *formulations for modelling heat transport in magnetised plasmas*, Journal of Computa-
722 tional Physics, 226 (2007), pp. 2306–2316, <https://doi.org/10.1016/j.jcp.2007.07.016>,
723 <http://www.sciencedirect.com/science/article/pii/S0021999107003166> (accessed 2014-08-
724 18).
- 725 [13] S. GÜNTER, Q. YU, J. KRÜGER, AND K. LACKNER, *Modelling of heat transport in magnetised*
726 *plasmas using non-aligned coordinates*, J. Comput. Phys., 209 (2005), pp. 354–370, <https://doi.org/10.1016/j.jcp.2005.03.021>,
727 <https://doi.org/10.1016/j.jcp.2005.03.021>, <http://dx.doi.org/10.1016/j.jcp.2005.03.021> (accessed
728 2013-06-06).
- 729 [14] S. JIN, *Asymptotic preserving (AP) schemes for multiscale kinetic and hyperbolic equations:*
730 *a review*, Lecture Notes for Summer School on "Methods and Models of Kinetic Theory"
731 June 2010, Rivista di Matematica della Università di Parma, (2012), pp. 177–206.
- 732 [15] A. LOZINSKI, J. NARSKI, AND C. NEGULESCU, *Numerical analysis of an asymptotic-preserving*
733 *scheme for anisotropic elliptic equations*, arXiv:1507.00879 [math], (2015), [http://arxiv.](http://arxiv.org/abs/1507.00879)
734 [org/abs/1507.00879](http://arxiv.org/abs/1507.00879) (accessed 2017-08-01). arXiv: 1507.00879.
- 735 [16] J. NARSKI AND M. OTTAVIANI, *Asymptotic Preserving scheme for strongly anisotropic*
736 *parabolic equations for arbitrary anisotropy direction*, Computer Physics Communica-

- 737 tions, 185 (2014), pp. 3189–3203, <https://doi.org/10.1016/j.cpc.2014.08.018>, <http://www.sciencedirect.com/science/article/pii/S0010465514002999> (accessed 2015-09-25).
- 738
- 739 [17] A. RATNANI, E. FRANCK, B. NKONGA, A. EKSAEVA, AND M. KAZAKOVA, *Anisotropic Diffusion*
- 740 *in Toroidal geometries*, ESAIM: Proceedings and Surveys, 53 (2016), pp. 77–98, <https://doi.org/10.1051/proc/201653006>, <http://www.esaim-proc.org/10.1051/proc/201653006>
- 741 (accessed 2016-08-19).
- 742
- 743 [18] P. SHARMA AND G. W. HAMMETT, *A fast semi-implicit method for anisotropic diffusion*, Jour-
- 744 *nal of Computational Physics*, 230 (2011), pp. 4899–4909, <https://doi.org/10.1016/j.jcp.2011.03.009>, <http://www.sciencedirect.com/science/article/pii/S0021999111001525> (ac-
- 745 cessed 2012-04-24).
- 746
- 747 [19] M. TANG AND Y. WANG, *An asymptotic preserving method for strongly anisotropic diffu-*
- 748 *sion equations based on field line integration*, *Journal of Computational Physics*, 330
- 749 (2017), pp. 735–748, <https://doi.org/10.1016/j.jcp.2016.10.062>, <http://www.sciencedirect.com/science/article/pii/S0021999116305708> (accessed 2016-12-18).
- 750
- 751 [20] B. VAN ES, B. KOREN, AND H. J. DE BLANK, *Finite-difference schemes for anisotropic diffusion*,
- 752 *Journal of Computational Physics*, 272 (2014), pp. 526–549, <https://doi.org/10.1016/j.jcp.2014.04.046>, <http://www.sciencedirect.com/science/article/pii/S0021999114003155> (ac-
- 753 cessed 2015-05-26).
- 754
- 755 [21] B. VAN ES, B. KOREN, AND H. J. DE BLANK, *Finite-volume scheme for anisotropic diffusion*,
- 756 *Journal of Computational Physics*, 306 (2016), pp. 422–442, <https://doi.org/10.1016/j.jcp.2015.11.041>, <http://www.sciencedirect.com/science/article/pii/S0021999115007810> (ac-
- 757 cessed 2017-08-01).
- 758
- 759 [22] C. YANG, J. CLAUSTRE, AND F. DELUZET, *Iterative solvers for elliptic problems with arbitrary*
- 760 *anisotropy strengths*. Submitted to SIAM Multiscale Modeling & Simulation.